Seasonal behavior of tropical to midlatitude upper tropospheric water vapor from UARS MLS

Brad J. Sandor,[1,2] William G. Read,[1] Joe W. Waters,[1] Karen H. Rosenlof[3]

Abstract. Measurements of upper tropospheric water vapor made during 1991-1997 with the Microwave Limb Sounder instrument on the Upper Atmospheric Research Satellite are described. Zonal mean results versus day of year are presented for tropical to midlatitudes on pressure surfaces 316, 215, and 147 hPa. The latitude of greatest upper tropospheric humidity (UTH) varies with season, following the Intertropical Convergence Zone. Annual maximum UTH occurs in northern summer at north tropical latitudes, coincident with the Indian monsoon and with a June-August maximum of water vapor transport to the lower stratosphere [*Rosenlof et al.*, 1997]. Comparison with lower stratospheric studies supports the *Rosenlof et al.* [1997] conclusion that water vapor transport is a maximum from the summer northern hemisphere tropical troposphere. Seasonally adjusted UTH is higher in the northern hemisphere than at equivalent southern hemisphere latitudes. The midlatitude secondary maximum in relative humidity seen in other (lower altitude) data sets is seen on the 316 hPa surface throughout the year, only in northern hemisphere spring-summer at 215 hPa, and does not occur at 147 hPa. These observations characterize seasonal and interhemispheric differences in strengths of midlatitude convection and of subtropical subsidence. Frequency distribution analysis of tropical measurements shows the peak (mode) of the frequency distribution to be much drier than mean and median values at 316 and 215 hPa and marginally drier than mean and median values at 147 hPa. The frequency distribution mode is drier in the tropical wet than in the dry season at 316 hPa, consistent with other data sets at 300-500 hPa [*Spencer and Braswell*, 1997; *Chiou et al.*, 1997] but is wetter in the tropical wet than in the dry season at 215 and 147 hPa. The wettest values of the frequency distribution mode occur in April-May, corresponding to neither the tropical wet nor the dry season.

1. Introduction

Upper tropospheric humidity (UTH) is of fundamental importance in understanding the Earth's atmosphere and climate. Water vapor is the most important greenhouse gas [*Manabe and Wetherald*, 1967; *Jones and Mitchell*, 1991], and it is in the upper troposphere that water vapor most strongly influences radiative forcing [*Udelhofen and Hartmann*, 1995]. Surface warming due to anthropogenic increases in CO_2 and other greenhouse gases is expected to occur with relative humidity remaining approximately constant, implying an increase in absolute humidity and consequent positive feedback to global warming [*Manabe and Wetherald*, 1967]. A representative modeling result [*Rind et al.*, 1991] is that water vapor feedback contributes ~40% of the global-average surface temperature increase in a doubled-CO_2 climate. An alternative scenario has been proposed [*Lindzen*, 1990] in which the increased convective activity due to CO_2 warming will dry the upper troposphere by shifting detrainment of air from convective plumes to a higher (colder) altitude. Because it is colder, the detrained air which spreads laterally through the upper troposphere would then be drier than without increased CO_2 abundance. The [*Lindzen*, 1990] scenario would thus provide a negative feedback to global warming. Satellite solar occultation observations of higher zonal mean summer than winter UTH values have been cited as evidence that enhanced convection moistens the upper troposphere [*Rind et al.*, 1991]. However, *Pierrehumbert* [1995] has argued that because of the nonlinear dependence of outgoing longwave radiation (OLR) on UTH, zonal mean UTH is less important for radiative

[1] Jet Propulsion Laboratory, California Institute of Technology, Pasadena.
[2] Now at National Center for Atmospheric Research, Boulder, Colorado.
[3] Cooperative Institute for Research in Environmental Sciences and NOAA Aeronomy Laboratory, Boulder, Colorado.

forcing than the dryness of and prevalence of the driest tropical UTH values. The importance of this issue is emphasized by observations of tropical 300-500 hPa UTH which show that the peak (mode) of the UTH frequency distribution is drier during the time of strongest tropical zonal mean convection (July) than the time of weakest tropical zonal mean convection (January) [Spencer and Braswell, 1997; Chiou et al., 1997]. Despite the importance of UTH, uncertainties in current values lead to uncertainties in calculated outgoing infrared flux from the troposphere comparable in magnitude to the change in outgoing IR flux calculated for a doubled-CO_2 atmosphere [Gutzler, 1993]. Accurate measurements of upper tropospheric humidity are important for assimilation into and validation of global climate models, both to understand the current climate and to predict correctly climate change.

Accurate measurements of upper troposphere water vapor are also important for understanding exchange between the troposphere and the stratosphere [Holton et al., 1995]. Transport of tropospheric water vapor to the lower stratosphere and oxidation of methane in the stratosphere are the dominant sources of water to the stratosphere, where it participates in ozone destruction both after freezing to form polar stratospheric clouds and after photochemical conversion to OH.

Microwave Limb Sounder (MLS) [Barath et al., 1993; Waters, 1993] has unique capabilities for measurement of UTH [Read et al., 1995]. Its limb-sounding geometry and wavelengths of observation allow retrieval of water vapor abundance at the pressure levels 147, 215, 316 and 464 hPa, a subset of the standard UARS "level 3" profile surfaces. (Standard UARS level 3 surfaces are pressure levels for which pressure is $P = 1000. \times 10^{-N/6}$ and integer values of N.) The UTH inversion problem is very nonlinear, and the estimated uncertainty and vertical resolution depend on the water vapor profile. Limb sampling is about 3 km and correlation length about 4 km in the troposphere, which gives typical single-profile absolute uncertainties of 20% (8 ppmv), 20% (25 ppmv), and 20% (125 ppmv) for the 147, 215, and 316 hPa levels, respectively, in units of relative humidity with respect to ice (and volume mixing ratio). Uncertainties in UTH averages over many profiles are much smaller, as indicated below by comparisons with other data sets in their regions of overlap. Single-profile measurement precision is better than 5% in relative humidity units. MLS altitude registration in the upper troposphere is better than that of nadir-sounding instruments, such as the TIROS operational vertical sounder (TOVS) measurements in broad pressure regimes 200-500 hPa, 300-700 hPa, and 600-1000 hPa [Soden and Bretherton, 1996]. MLS observations are less sensitive to interference by cirrus cloud and aerosol than observations at infrared and visible wavelengths. They also have better latitude coverage and more frequent observations than occultation experiments such as the Stratospheric Aerosol and Gas Experiment II (SAGE II) [Larsen et

al., 1993; Chiou et al., 1997]. Regular in situ humidity measurements are made from operational radiosondes [Peixoto and Oort, 1996] but are usually restricted to pressures greater than 300 hPa by instrumental limitations and are sparse in remote oceanic regions. Advantages of high vertical resolution, near global coverage with 1300 profiles per day, and relative insensitivity to aerosol (cirrus and volcanic) contamination make MLS a valuable new system for measuring UTH.

MLS UTH initial observations and retrieval techniques are described by Read et al. [1995], who also present preliminary scientific results at 215 hPa. Read et al. [1995] demonstrate the usefulness of MLS UTH observations for measurements of zonal mean behavior, tracking large-scale weather systems, and mapping seasonal behavior on $4° \times 4°$ horizontal scales. A more detailed study of 215 hPa zonal mean behavior is presented by Elson et al. [1996], in parallel with a similar study of stratospheric water vapor. Stone et al. [1996] present a case study of baroclinic wave activity from its signature in the 215 hPa MLS UTH data.

In the current study, initial results of an improved retrieval scheme for MLS UTH are described. Zonal mean global MLS UTH measurements from a 5 year data set are analyzed for seasonal variability on 316, 215, and 147 hPa pressure surfaces and tropical to midlatitudes and discussed in the context of lower-altitude TOVS [Soden and Bretherton, 1996] and higher-altitude Halogen Occultation Experiment (HALOE) [Rosenlof et al., 1997] data. Monthly frequency distributions of UTH values are presented for 30°S-30°N on these pressure levels and compared with lower-altitude UTH frequency distributions [Spencer and Braswell, 1997; Chiou et al., 1997].

2. Observations

The initial MLS UTH retrieval described by Read et al. [1995] has been improved by using better characterization of the dry and wet absorption continua, and including field of view and refractive effects, combined with an iterated optimal estimation retrieval. This new retrieval (W.G. Read et al., manuscript in preparation, 1998), which has produced the MLS Version 4 data product for public use, provides UTH on 464, 316, 215, and 147 hPa pressure surfaces. ("Version 4" is the most current and best data set for all MLS-measured geophysical parameters.) Figure 1 shows the nearly linear plus bias relationship, on each of four pressure surfaces, between Version 4 UTH data and UTH values obtained with the Read et al. [1995] preliminary retrieval. The functions shown in Figure 1 are best fits to scatterplots of Version 4 data versus preliminary [Read et al., 1995] data, obtained from a profile-by-profile comparison between Version 4 and preliminary values for 62 days of data (21 days in June 8 to July 3, 1994; 32 days in November 25, 1995 to March 1, 1996, and 9 additional days distributed through 1991-1995) and are valid for
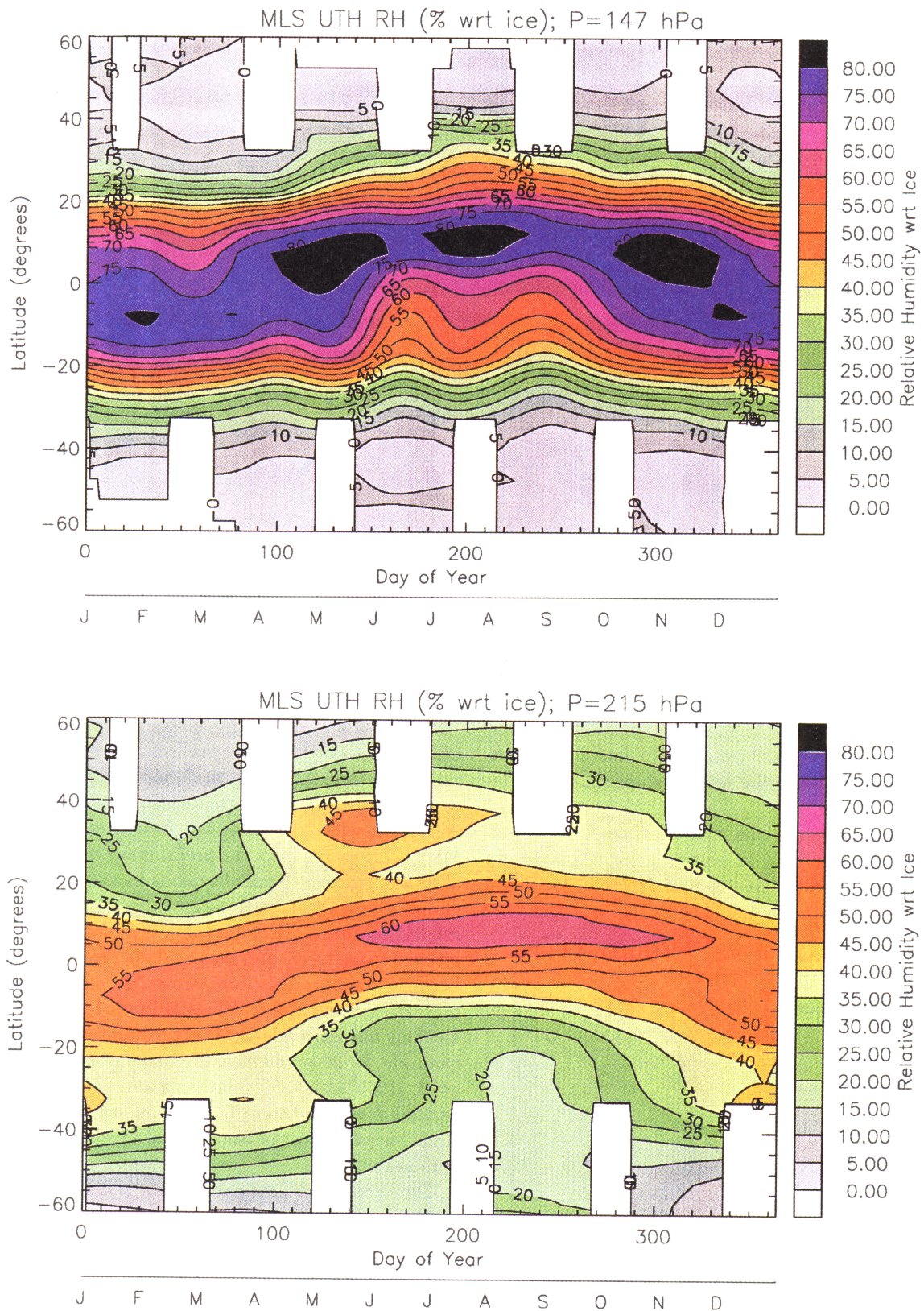
Plate 1. Relative humidity with respect to ice on pressure surfaces at (a) 147, (b) 215, and (c) 316 hPa as measured with the UARS MLS instrument. An 8 day Gaussian smoothing has been applied to suppress short-term variability and data from September 1991 to June 1997 averaged to determine mean seasonal behavior. The 1991-1997 average most strongly represents the first half of this time period, due to the decrease in measurement frequency associated with increasing age of UARS.
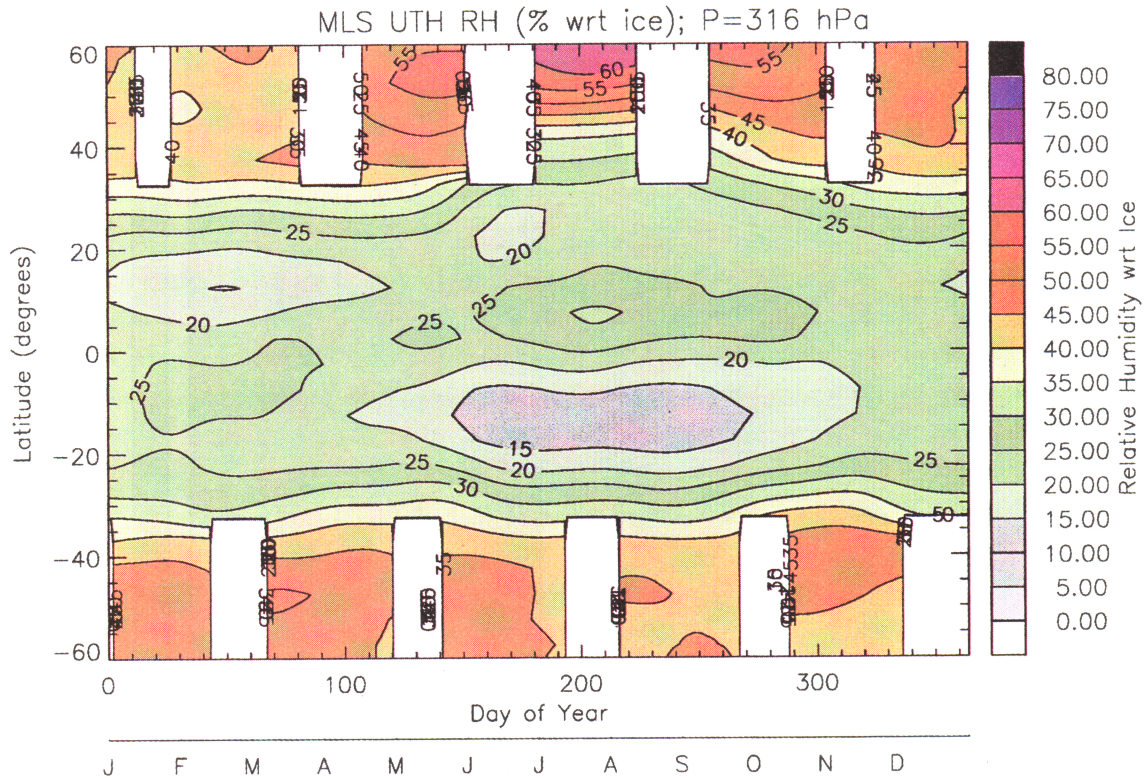
Plate 1. (continued)

UTH mixing ratios ≤500 ppmv. No latitude dependence has been found to the relationships shown in Figure 1.

At 147 and 464 hPa the new Version 4 UTH values are always drier than those presented in previously published MLS studies. At 215 and 316 hPa, Version 4

Figure 1. Relationship between the updated Version 4 MLS UTH retrieved values and MLS UTH retrieved with the preliminary algorithm [*Read et al.*, 1995]. The functions are piecewise linear best fits to scatterplots of Version 4 versus preliminary [*Read et al.*, 1995] values for each pressure level.

UTH values are drier than preliminary values for mixing ratios less than 220 ppmv and moister than preliminary values for mixing ratios greater than 220 ppmv. This is consistent with conclusions of *Newell et al.* [1996] that MLS UTH values from the preliminary retrieval were biased wet relative to simultaneous in situ measurements made from a DC-8, with largest discrepancies at smallest mixing ratios. Because there is a piecewise linear relationship between previous and current retrievals and because the current values are strictly increasing with increasing preliminary values (Figure 1), previous conclusions based on relative UTH values remain valid. For example, 80-90 ppmv measurements presented by *Stone et al.* [1996] at 40°-60°S latitude and 215 hPa should be revised downward to ~25-35 ppmv, a factor of 3 reduction, but the wave pattern *Stone et al.* [1996] analyze is maintained.

The Version 4 standard MLS UTH product is in units of relative humidity with respect to ice (RHI). The data discussion below is also primarily in terms of RHI, with conversion from mixing ratio units done using National Meteorological Center (NMC) temperature values, which are placed in the MLS data files at the standard UARS pressure levels [*Fishbein et al.*, 1996]. Presentation of data in units of relative humidity has the following advantages: (1) There is immediate physical meaning in terms of the relationship between vapor and ice. Retrieved values above 100% indicate the likely presence of cirrus cloud. (2) RHI values are
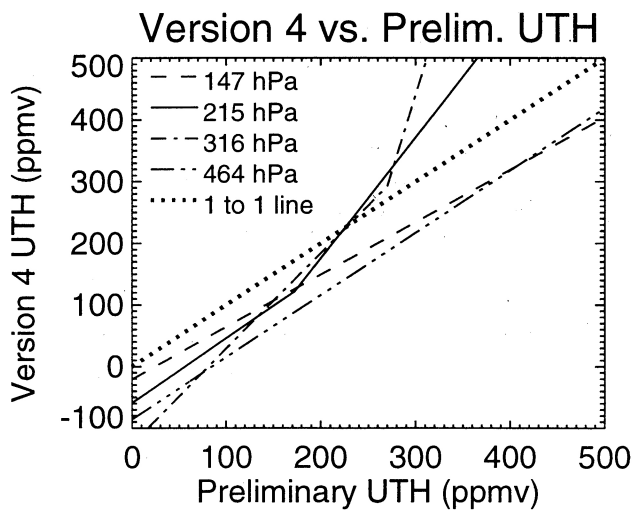
easier to quickly compare with traditional tropospheric data sets such as those from sondes and IR satellites. (3) Because relative humidity changes more slowly with altitude than the mixing ratio, interpolation between measurements in RHI units provides a more accurate profile shape.

RHI units are most appropriate for low and midlatitudes but for the MLS retrieval have the disadvantage of deemphasizing latitudes higher than ∼50°, where all three pressure surfaces are usually in the lower stratosphere [Holton et al., 1995; Appenzeller et al., 1996]. Retrieved H_2O mixing ratios in these regions are very low, and the dependence of mixing ratio on altitude is relatively weak, consistent with stratospheric behavior. In the present work, zonal mean relative humidities less than ∼5% are not discussed, and this is the determining factor in the high-latitude cutoffs of the data presentation. In cases involving high-latitude studies, mixing ratio units may be preferred. Mixing ratio or relative humidity with respect to liquid (RHL) are preferred when making comparison with data sets reported in those units and are readily obtained from MLS RHI values with use of coincident temperatures.

As a preliminary validation of the MLS data, Figures 2 and 3 present comparisons with balloon sonde [Elliott and Gaffen, 1991; Larsen et al., 1993] and SAGE II [Chiou et al., 1997] data, respectively. Sonde measurements are from a global network of 2-4 times daily balloon launches at land-based meteorological stations. Figure 2 presents the average of MLS and sonde measurements from the the same 62 days used to derive
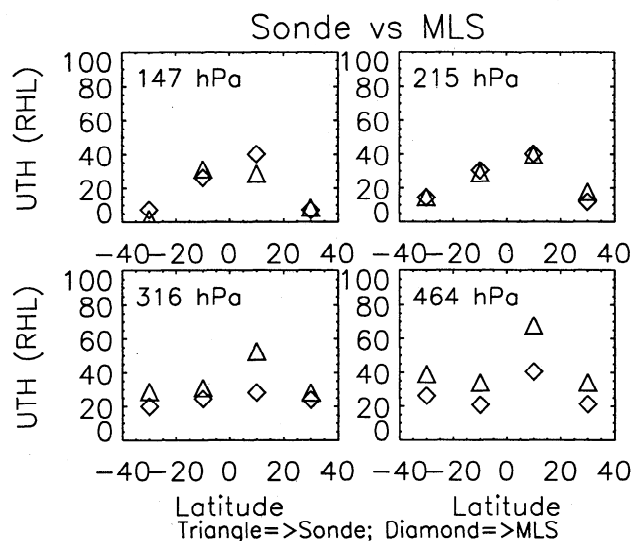
the functions shown in Figure 1, where MLS and sonde measurements are coincident within 2° latitude, 2° longitude, and 3 hours time. MLS-retrieved values greater than 100% (which occur only in the 0°-20°N, 147 hPa bin of Figure 2) have been set to 100% for comparison as a way to account for ice contamination. Sonde measurements are least accurate in the cold, dry conditions typical of the upper troposphere and display systematic biases among instrument types. To minimize these problems, Figure 2 includes sonde data from a single instrument type, the thin film capacitor, chosen because it is the instrument type most reliable in the upper troposphere [e.g., Larsen et al., 1993]. Figure 2 shows MLS to be consistently drier than sonde measurements at 316 and 464 hPa. Sensitivity studies to date indicate that the MLS relative humidity values should be accurate to 20% or better, with individual profile measurement precision better than 5%. (See section 1 for more detailed discussion of measurement uncertainty.) At 147 and 215 hPa the sonde and MLS measurements display no systematic offset. MLS measurements reflect conditions along the ∼100 km line of sight, while the in situ sonde measurements sample a very small volume of air, and the MLS versus sonde coincidence criteria allow measurement separations that are large relative to true atmospheric variability, which lead to a large range of point-by-point differences between MLS and sonde measurements.

Figure 3 compares zonal mean seasonal UTH measurements between SAGE II [Chiou et al., 1997] and MLS. The SAGE II data are from a 5.5 year measurement period ending in May 1991, prior to the eruption of Mount Pinatubo. Sulfate aerosol from that eruption interferes with later SAGE II measurements. The MLS values, which are not sensitive to volcanic aerosol, are from the period September 1991 (start of mission) to June 1997 (date of battery failure and consequent pointing degradation due to insufficient power to operate the 63 GHz radiometer). Zonal mean UTH is higher in the MLS than the SAGE II data, with biggest differences at the highest mixing ratios. This is consistent, because MLS measurements are taken even in the presence of cirrus clouds, while SAGE II measurements represent only cases under clear-sky situations. MLS data in Figure 3 reflect seasonal movement of the zonal mean Intertropical Convergence Zone (ITCZ), in that highest mixing ratios are north of the equator in JJA and south of the equator in DJF. SAGE II does not clearly show this ITCZ behavior.

In section 3, MLS UTH zonal mean seasonal behavior is presented and discussed in relation to results derived from infrared nadir-looking observations made with the TOVS [Soden and Bretherton, 1996] and with in situ balloon-borne measurements [Peixoto and Oort, 1996], each most accurate at altitudes below those sampled with MLS. MLS data are consistent with these measurements and extend them to higher altitudes where water vapor behavior is qualitatively different. We

Figure 2. Comparison of average results of coincident balloon sonde and MLS UTH determinations from the same 62 days used to establish the relationships in Figure 1. Each point shown is the average of measurements meeting coincidence criteria (see text) within a 20° latitude range. For latitude bins 40°S-20°S, 20°S-0°, 0°-20°N, and 20°N-40°N the numbers of coincidences are 20, 5, 28, and 52, respectively.

also discuss MLS UTH data in relation to the HALOE measurements of lower-stratospheric water vapor [*Russell et al.*, 1993; *Harries et al.*, 1996]. Seasonal variation in tropical UTH values is shown to be compatible with the seasonal variation and hemispheric asymmetry seen in lower-stratospheric water vapor [*Rosenlof et al.*, 1997]. In section 4, monthly frequency distributions are presented for tropical (30°S-30°N) latitudes and compared with microwave (183 GHz) nadir-looking observations made with the Special Sensor Microwave humidity sounder (SSM/T-2) at lower altitudes [*Spencer and Braswell*, 1997] and with the *Chiou et al.* [1997] frequency distribution analysis of SAGE II UTH data.

3. Zonal Mean Seasonal Behavior

UTH measurements from the September 1991 start of the UARS mission to June 1997 are presented in Plate 1 for pressure levels 147, 215, and 316 hPa. An 8 day Gaussian smoothing algorithm has been applied to suppress effects of short-term variability (i.e., weather), and data have been binned by day of year to display seasonal behavior. These procedures lead to complete temporal coverage for latitudes 34°S to 34°N. The UARS satellite operations dictate that MLS alternate between observing latitudes 34°N-80°S for one ~36 day period and 34°S-80°N for the next ~36 days, resulting in periodic data gaps at latitudes poleward of 34°.

Contours of constant relative humidity shift in latitude, following the Sun with a lag of about 2 months. Maximum tropical UTH on each pressure level oscillates between approximately 10°S and 10°N, following the annual motion of the Intertropical Convergence Zone (ITCZ) associated with the ascending branch of the Hadley cell. This seasonal shifting of the ITCZ is also seen in sonde [*Peixoto and Oort*, 1996], TOVS [*Soden and Bretherton*, 1996], and SAGE II [*Rind et al.*, 1993] data sets. Longitudinally resolved analyses of the MLS data, showing seasonal motion of the ITCZ, have been presented by *Read et al.* [1995] and *Newell et al.* [1997]. At fixed latitudes lower than 15°, two local maxima are seen in the annual cycle, corresponding to north and south shifting of the ITCZ. The two maxima are most clear at 147 hPa for 0°-10°N of the equator, where the UTH cycle is largely semiannual (Plates 1a and 2a). This agrees with the *Newell et al.* [1997] harmonic analysis, showing the semiannual component of 147 hPa UTH variation is strongest at about 5°N. For latitudes higher than about 15°, a single maximum value occurs during late spring to late summer. Relative humidity values in the northern extratropics are generally higher than seasonally adjusted values at the equivalent southern extratropical latitudes (Plates 1 and 2) (as expected from the stronger convection over continents than over oceans), in agreement with lower-altitude data sets [e.g., *Soden and Bretherton*, 1996] and with the *Elson et al.* [1996] 215 hPa absolute humid-
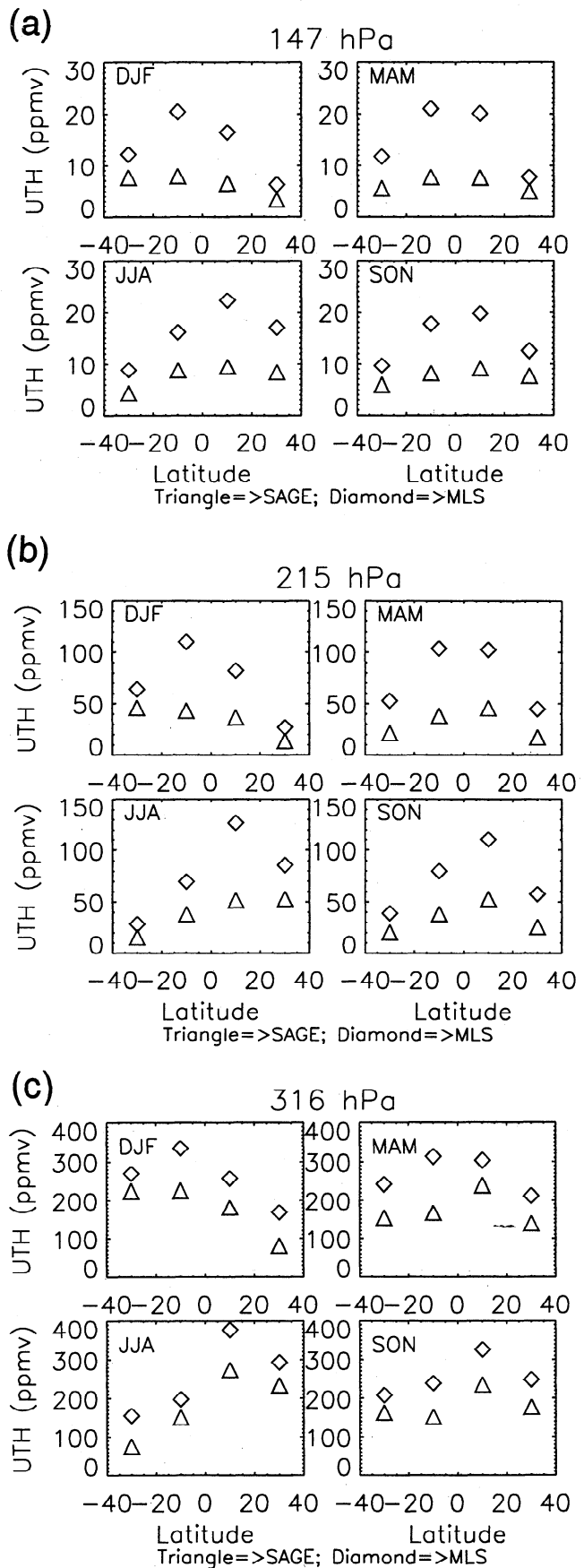

Figure 3. Comparison of zonal mean SAGE II [*Chiou et al.*, 1997] and MLS UTH values for (a) 147 hPa, (b) 215 hPa, (c) 316 hPa.

ity analysis. Plate 3 shows absolute humidity (mixing ratio) at 147 hPa. Similar high-latitude asymmetry in UTH has been reported [Kelly et al., 1991], though the mechanisms underlying hemispheric asymmetry at high and low latitudes may be quite different.

Plates 2a and 2b present RHI values as a function of day of year and altitude, for 5°-10°N and 5°-10°S latitude, respectively. It is clear that for these latitude bins the southern hemisphere is drier than the northern hemisphere at seasonally equivalent dates. Plate 2a displays two 147 hPa maxima, in May-June and in October-November, separated by a strong minimum in February and a weaker minimum in August.

Within the ITCZ, maximum relative humidity values on the 215 and 316 hPa surfaces (Plates 1b, 1c) occur in July at 5°-15°N, in agreement with the Soden and Bretherton [1996] 500-200 hPa result. At 147 hPa (Plate 1a) the RHI maximum in the ITCZ is less well defined, extending from April to November. UTH mixing ratio maxima are in the ITCZ during May to August on all three pressure surfaces. Plate 3 for example, shows mixing ratios at 147 hPa, with maximum values in May-August at the latitude of the ITCZ. This agrees with the [Newell et al., 1997] conclusion from the preliminary MLS UTH retrieval [Read et al., 1995] that UTH is an overall maximum in July-August, associated with the intense Indian monsoon moisture plume. North of 15°N, maximum 147 hPa RHI occurs in July. South of the equator, maximum 147 hPa RHI occurs in January to February. Thus at subtropical to midlatitudes in both hemispheres the 147 hPa water vapor maxima occur about a month after summer solstice. This is in contrast to the behavior in the lower stratosphere where the subtropical water vapor maximum in both hemispheres occurs during the June-August period; a consequence of the annual cycle in tropical tropopause temperatures [Mote et al., 1996]. However, the 147 hPa behavior is consistent with the Rosenlof et al. [1997] hemispheric asymmetry analysis which showed more water being pumped into the northern hemisphere summer stratosphere (June-August, tropical wet period) than into the southern hemisphere summer stratosphere (December-February, tropical dry period). The Rosenlof et al. [1997] presentation of HALOE water vapor [Russell et al., 1993; Harries et al., 1996] on the 390 K potential temperature surface (~100 hPa) shows maximum mixing ratios in July to August for 10°-50°N but in October to November for 10°-50°S. In the tropical northern hemisphere the maximum in stratospheric water vapor (seen in HALOE data) occurs about a month after maximum in UTH (seen in MLS data). In the tropical southern hemisphere the maximum in stratospheric water vapor occurs 10 months after the maximum in UTH, while the minimum in southern hemisphere stratospheric water vapor occurs 1-2 months after the southern hemisphere UTH maximum. Thus seasonal H_2O maxima in the upper troposphere and lower stratosphere are nearly simultaneous at north tropical latitudes but well sepa-

rated in time at south tropical latitudes. These observations support the idea that the lower stratosphere is supplied with water directly from the upper troposphere in the northern hemisphere during summer but not in the southern hemisphere. The maximum entry of tropospheric water vapor to the stratosphere occurs at the time of maximum tropical tropospheric water mixing ratios, as well as at the time of maximum tropical tropopause temperatures [Mote et al., 1996].

Throughout the year the TOVS nadir-sounding data [Soden and Bretherton, 1996] display 200-500 hPa UTH maxima at the ITCZ and at midlatitude storm tracks, with intervening subtropical minima 20°-30° north and south of the ITCZ. MLS measures similar subtropical minima in RHI (Plate 1), located 20°-30° north and south of the ITCZ on the 316 and 215 hPa pressure surfaces. This structure is prevalent through the year at 316 hPa and distinct at 215 hPa only in the northern hemisphere during May-August. It is not seen at 147 hPa, where RHI decreases monotonically with latitude from the ITCZ to midlatitudes throughout the year. The qualitative agreement between UTH behaviors seen in TOVS 200-500 hPa data and MLS 316 hPa data provides some validation of each measurement system. The MLS data at 215 and 147 hPa depict a transition away from lower-altitude behavior. The absence of a subtropical minimum at 147 hPa suggests the zonal mean midlatitude convection is not deep enough to produce a secondary maximum in UTH. The seasonal behavior at 215 hPa suggests midlatitude convection is strong enough to produce a secondary UTH maximum only during northern hemisphere spring-summer, in association with the seasonal maximum in solar heating. The stronger northern than southern hemisphere midlatitude secondary maximum is consistent with the stronger convection associated with northern hemisphere landmasses, the same reason the northern hemisphere UTH values are higher than those south of the equator. Northern hemisphere summer corresponds to the tropical wet period, and the presence of a subtropical RHI minimum in May-August may be enhanced by subsidence driven by the maximum in tropical upwelling. In contrast to the relative-humidity behavior, absolute humidity (mixing ratio) is strictly decreasing with latitude away from the ITCZ maximum on all three pressure surfaces at all times of the year (e.g. Plate 3), consistent with the 215 hPa absolute humidity analysis of Elson et al. [1996]. This illustrates an important point that qualitative statements about UTH, such as timing and location of maximum values, are often dependent on whether relative humidity or mixing ratio units are used.

4. Frequency Distribution of Tropical Humidity

To understand the influence of UTH on OLR, it is important to measure not only the zonal mean values discussed above but also the frequency distribution of
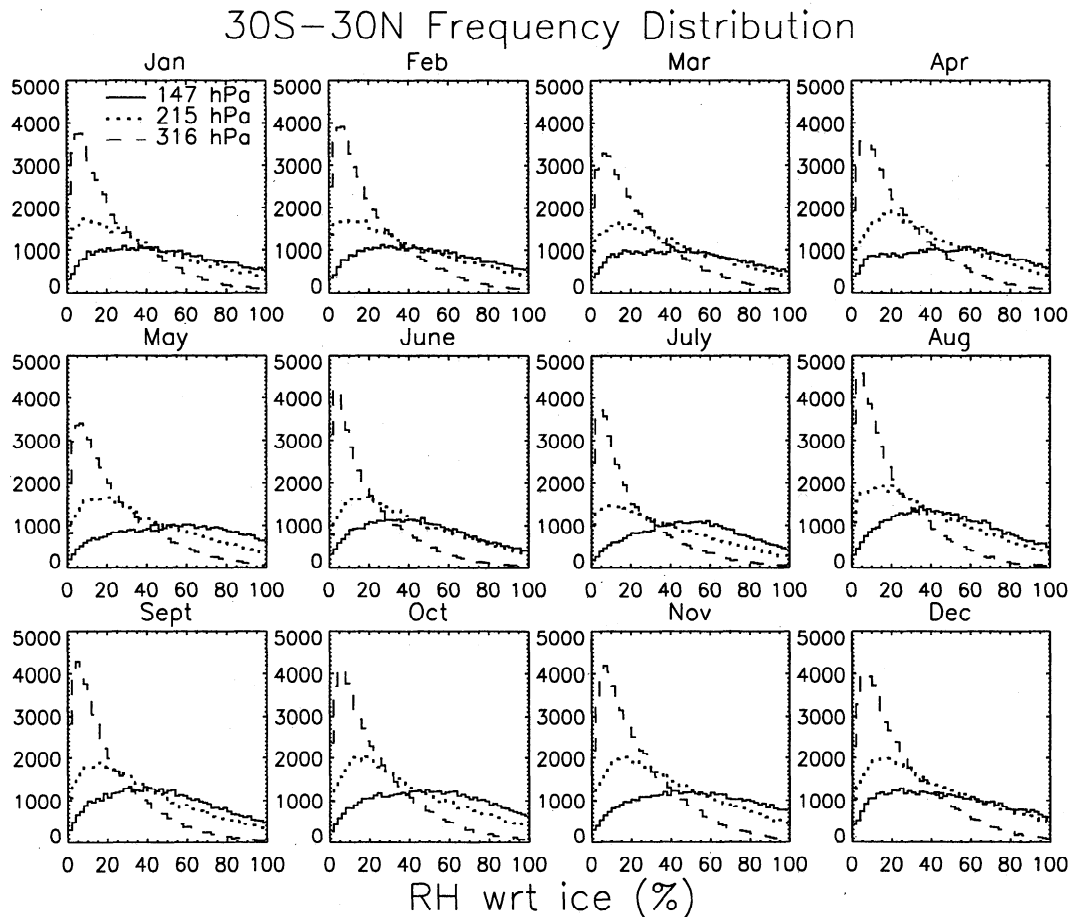
30S-30N Frequency Distribution

Figure 4. Monthly (1991-1997) frequency distributions for MLS measurements of 30°N-30°S RHI.

UTH abundances. Because of the nonlinear dependence of OLR on UTH the driest tropospheric regions act as "radiator fins" [*Pierrehumbert*, 1995] where much of the tropical radiative heat loss to space occurs. Understanding these driest regions, and in particular predicting their response to increasing CO_2 abundances, is important for determining the relative roles of radiative cooling to space and meridional transport to mid-latitudes as mechanisms for heat loss from the tropics. *Spencer and Braswell* [1997] present such a relative humidity frequency analysis, based on data from the SSM/T-2, a satellite-borne nadir-looking microwave instrument. SSM/T-2 has three water vapor channels, with broad altitude weighting functions similar to those of the TOVS IR nadir-sounder discussed above. The three channels of SSM/T-2 are sensitive to water vapor for altitude regimes at 250-450 hPa, 350-600 hPa, and 400-750 hPa in wet conditions and altitudes at ~100 hPa higher pressures under dry conditions. *Spencer and Braswell* [1997] perform a frequency analysis showing peaks (mode values) in the 300-500 hPa, 30°S-30°N, RHL distribution at 9% and 6% in January and July 1994, respectively; that is, the peak in (mode of) the tropical RHL frequency distribution is drier during the tropical wet than dry season. The SSM/T-2 30°S-30°N

data show frequency peaks at about RHL=11% for 400-650 hPa and 20% for 450-800 hPa, with no clear difference between January and July peaks. *Chiou et al.* [1997] present a similar frequency analysis, comparing SAGE II data for DJF with JJA for 300 hPa, albeit at lower RHL resolution (~5%) than that of the SSM/T-2 analysis (1%). Equatorward of 30°, the SAGE II frequency distribution peak is at 10% in DJF, and 7.5% in JJA, similar to the SSM/T-2 January versus July 300-500 hPa result.

Figure 4 shows the monthly frequency distributions of MLS RHI values for latitudes 30°S-30°N. Values are from the years 1991-1997, and total number of measurements varies from month to month. The sharp peaks in the 316 and 215 hPa frequency distributions are necessarily made less sharp by random error in MLS measurements, as they would be by any other measurement system. The large number of occurrences of low relative humidities are spread by random error into a Gaussian envelope. For this reason and because the sharp peaks in the 316 and 215 hPa frequency distributions are at such low relative humidities, it is likely that the true number of values in the driest (0% to 2%) histogram bins shown in Figure 4 is smaller than the measured number of values in this bin. Figure 5 shows mean, me-
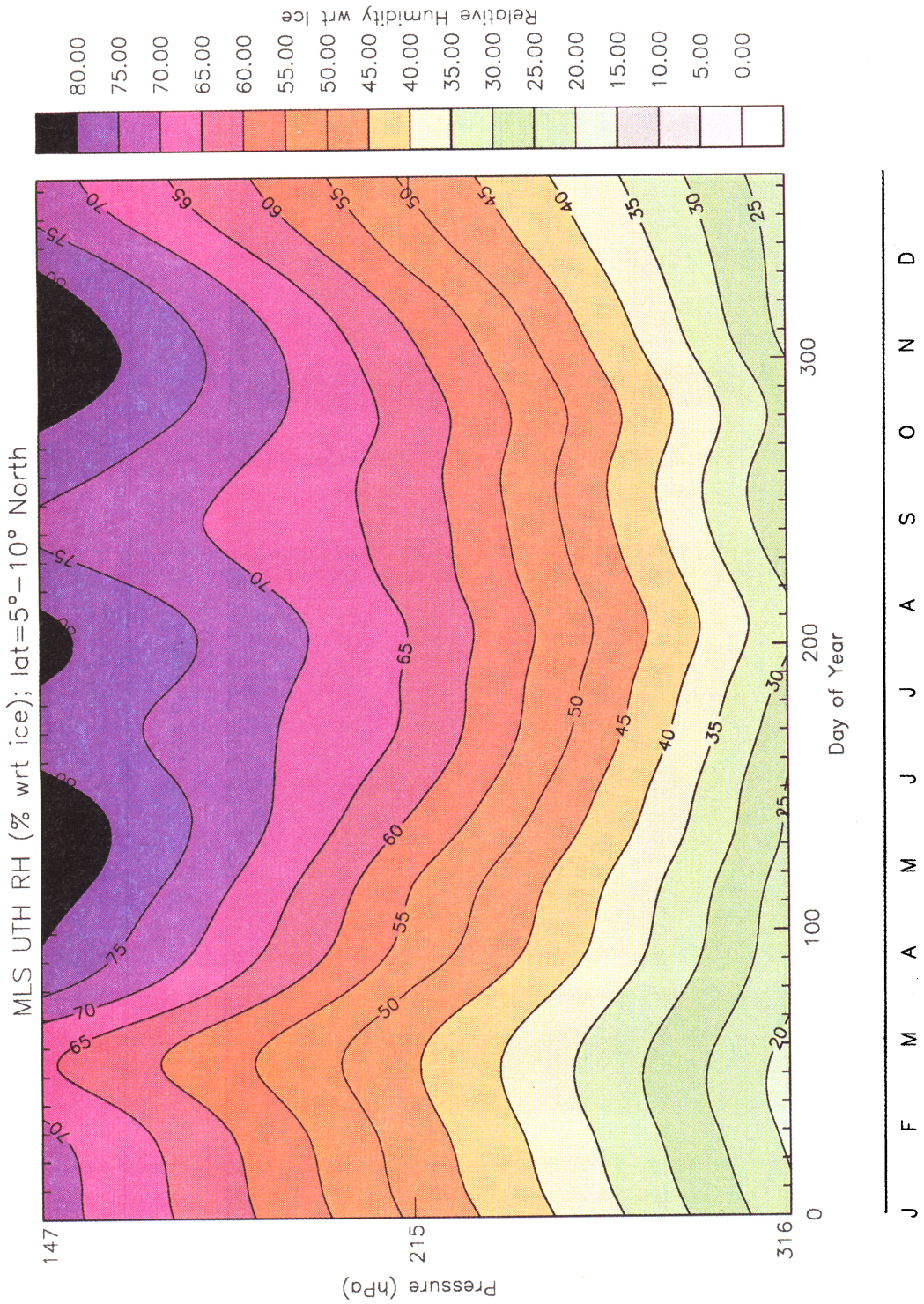
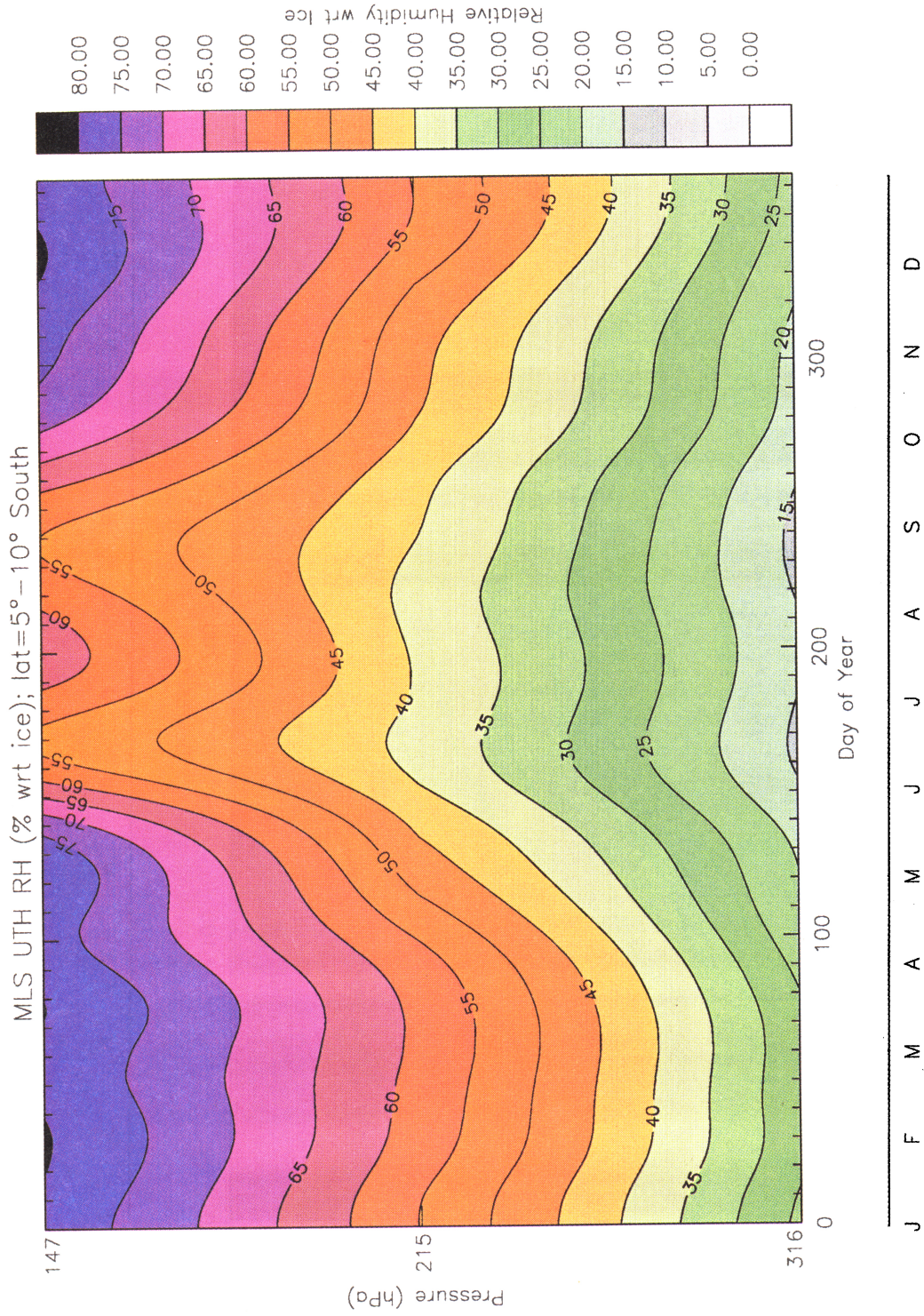**Plate 2.** Relative humidity with respect to ice at latitudes (a) 5°-10°N and (b) 5°-10°S.
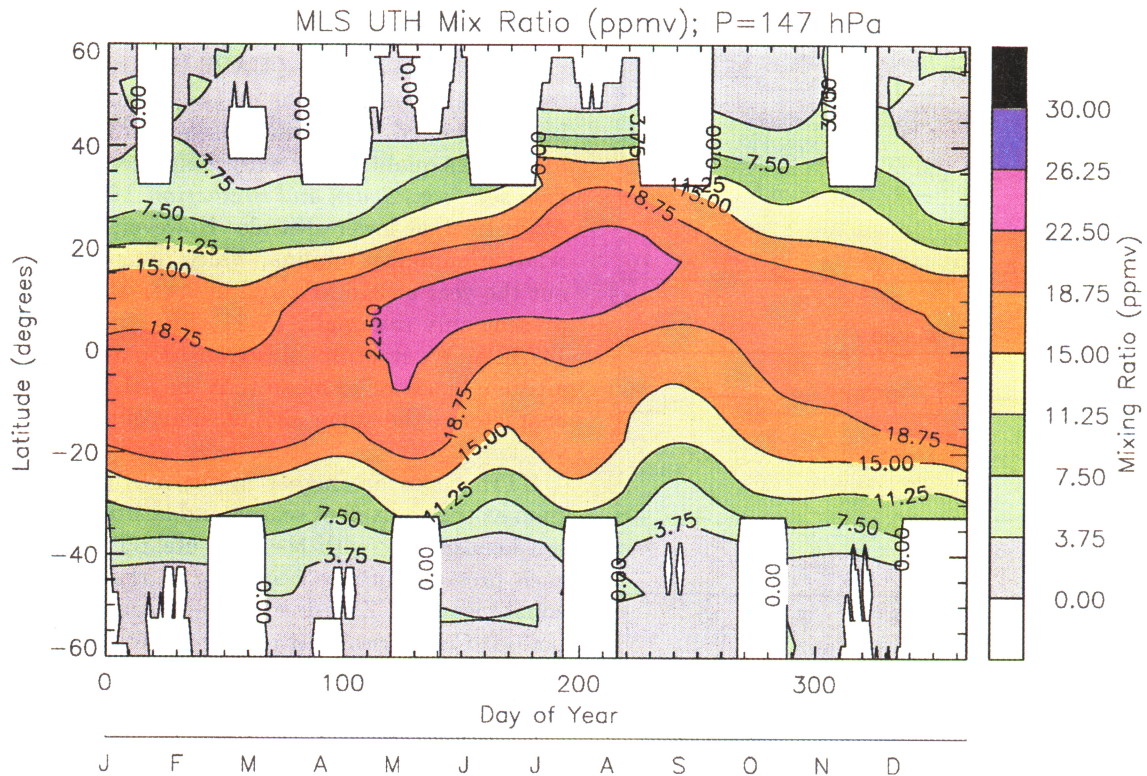
Plate 2. (continued)

Plate 3. Same data as Plate 1a but in mixing ratio units. Note that maximum in mixing ratio units occurs in May-August, while maximum in RHI units occurs throughout the year.

dian, and mode values versus month of year for RHI at 30°S-30°N latitude determined from the MLS measurements at 147, 215, and 316 hPa. Mean values for this latitude range are lowest at 316 hPa, highest at 147 hPa, and monthly mean values vary by less than 10% from the annual mean at each pressure level. Monthly median values follow a similar pattern. Monthly mode values are more variable, ranging from 25% to 59% at 147 hPa and from 7% to 21% at 215 hPa. The general shape of the 316 and 215 hPa MLS UTH frequency distributions is similar to that seen in the SSM/T-2 data [*Spencer and Braswell*, 1997] and SAGE II [*Chiou et al.*, 1997] data, in that the mode values are significantly drier than the mean and median. At 147 hPa this is less distinct, with monthly mode values smaller than mean and median values for only 9 months of the year. *Spencer and Braswell* [1997] show mode values in the frequency distributions for January and July 1994 to become drier with increasing altitude up to their highest (300-500 hPa) altitude bin. MLS UTH values show the reverse trend from 316 to 147 hPa (Figure 5c); mode values increase with altitude.

Values of the frequency distribution mode for 30°S-30°N at comparable altitudes are similar among the tropical wet (JJA) versus dry (DJF) period analyses of SSM/T-2 [*Spencer and Braswell*, 1997], SAGE II [*Chiou et al.*, 1997], and MLS [this work] data. SSM/T-2 300-500 hPa data show RHL modes of 6% in July and 9%

in January; MLS 316 hPa data show RHL modes of 3% in July and 5% in January. SAGE II 300 hPa data (reported on a 5% grid) have modes 7.5% in JJA and 10% in DJF; MLS 316 hPa RHL have modes 3% in JJA and 5% in DJF. Like SSM/T-2 [*Spencer and Braswell*, 1997] and SAGE II [*Chiou et al.*, 1997] data, MLS data show a drier mode during the tropical wet period than the dry period at 316 hPa. This agreement provides some validation of the three data sets.

We have extended the MLS analysis to higher altitudes and throughout the year. The increase with altitude of RHI mean, median, and mode values above 316 hPa parallels the behavior of the mean reported in other studies [e.g., *Newell et al.*, 1997, their Figure 5]. This can be understood in the context that high relative humidities occur near the tops of convective systems, which for strong tropical systems could be near 147 hPa, and subsidence to lower altitudes decreases relative humidity below the convective canopies due to adiabatic warming.

While the mode value at 316 hPa is drier in the tropical wet period than in the dry period (RHI= 5% in JJA, 7% in DJF), Figure 5c shows the reverse is true at 215 hPa (RHI= 18% in JJA, 12% in DJF) and at 147 hPa (RHI= 47% in JJA, 27% in DJF). At 215 and 147 hPa the mode is wetter in the tropical wet period than in the dry period.

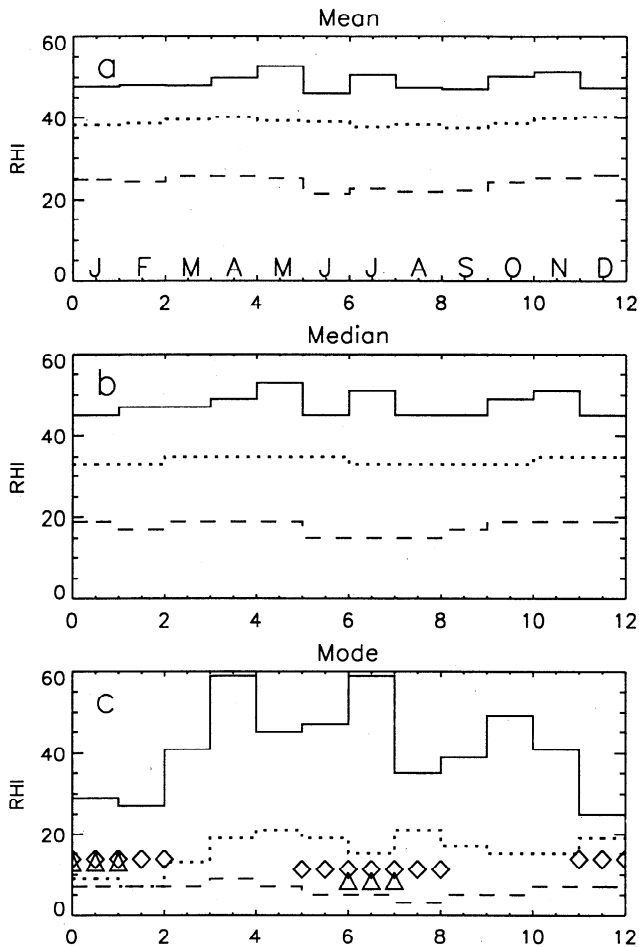Figure 5c shows that for all three pressure levels the

Figure 5. Monthly variation of the (a) mean, (b) median, and (c) mode of the frequency distributions shown in Figure 4. RH is with respect to ice. The solid histogram indicates MLS values at 147 hPa, the dotted histogram indicates MLS values at 215 hPa, and the dashed histogram indicates MLS values at 316 hPa. Diamonds indicate mode values from SAGE II at 300 hPa [Chiou et al., 1997], and triangles indicate mode values at 300-500 hPa from SSM/T-2 [Spencer and Braswell, 1997].

MAM period also has maximum monthly mode values. At 316 hPa the wettest monthly mode value occurs in April. At 215 hPa, maximum monthly mode values occur in May and August. At 147 hPa, maximum monthly mode values occur in April and July. The high mode values in April and May may be associated with the annual maximum in lower-altitude meridional convergence of water vapor that occurs in April [Rasmusson, 1972]. Newell et al., [1997] have discussed this meridional convergence in the context of longitudinally resolved monthly mean MLS water vapor measurements. Because MAM corresponds to neither the tropical wet nor the dry period, these results demonstrate the need for full seasonal analyses of the UTH frequency distribution at multiple altitudes. Characterization of UTH based on a wet versus dry season analysis in a single altitude bin is not sufficient.

5. Summary

Results of an improved UARS MLS retrieval of upper tropospheric water vapor at low to midlatitudes have been presented. Zonal mean seasonal behavior at 316 hPa agrees qualitatively with the patterns seen in other data sets [e.g., Soden and Bretherton, 1996; Peixoto and Oort, 1996] at lower altitude. However, the subtropical relative humidity minima, which are present throughout the year at 316 hPa and in lower-altitude data, are present only seasonally at 215 hPa and are absent at 147 hPa. We interpret this transition away from lower-altitude behavior to mean that the MLS measurements characterize the upper altitude limit of midlatitude convection.

UTH values are higher in the northern hemisphere than at the equivalent season and latitude in the southern hemisphere, with the absolute UTH maximum on each pressure surface occurring at the latitude of the zonal mean ITCZ during the June-August tropical wet period. Comparison with lower-stratospheric water vapor data shows that the seasonal H_2O maxima in the upper troposphere and lower stratosphere are simultaneous at north tropical latitudes but well separated in time at south tropical latitudes, consistent with the Rosenlof et al. [1997] hemispheric asymmetry analysis.

A UTH frequency distribution analysis of 30°S-30°N MLS data shows mode values are much drier than mean and median values at 316 and 215 hPa, similar to the nadir-sounding SSM/T-2 observations at lower altitudes [Spencer and Braswell, 1997], and to the 300 hPa SAGE II limb-sounding data [Chiou et al., 1997]. At 147 hPa the 30°S-30°N mode values are marginally drier than mean and median values. The peak (mode) in this frequency distribution is drier in the tropical wet season (June-August) than in the tropical dry season (December-February) at 316 hPa but wetter in the wet season than dry season at 215 and 147 hPa. Wettest values of the UTH frequency distribution peak also occur in April-May, corresponding to neither the tropical wet (JJA) nor the dry (DJF) periods. MLS measurements thus show that the dryness and frequency distribution of the driest tropical UTH values are complex functions of altitude and season.

References

Appenzeller, C., J.R. Holton, and K.H. Rosenlof, Seasonal variation of mass transport across the tropopause, J. Geophys. Res., 101, 15,071-15,078, 1996.

Barath, F.T., et al., The Upper Atmospheric Research Satellite Microwave Limb Sounder instrument, *J. Geophys. Res.*, *98*, 10,751–10,762, 1993.

Chiou, E.W., M.P. McCormick, and W.P. Chu, Global water vapor distributions in the stratosphere and upper troposphere derived from 5.5 years of SAGE II observations (1986-1991), *J. Geophys. Res.*, *102*, 19,105–19,118, 1997.

Elliott, W.P., and D.J. Gaffen, On the utility of radiosonde humidity archives for climate studies, *Bull. Am. Meteorol. Soc.*, *72*, 1507–1520, 1991.

Elson, L.S., W.G. Read, J.W. Waters, P.W. Mote, J.S. Kinnersley, and R.S. Harwood, Space-time variations in water vapor as observed by the UARS Microwave Limb Sounder, *J. Geophys. Res.*, *101*, 9001–9015, 1996.

Fishbein, E.F., et al., Validation of UARS Microwave Limb Sounder temperature and pressure measurements, *J. Geophys. Res.*, *101*, 9983–10,016, 1996.

Gutzler, D.S., Uncertainties in climatological tropical humidity profiles: Some implications for estimating the greenhouse effect, *J. Clim.*, *6*, 978–982, 1993.

Harries, J.E., J.M. Russell III, A.F. Tuck, L.L. Gordley, P. Purcell, K. Stone, R.M. Bevilacqua, M. Gunson, G. Nedoluha, and W.A. Traub, Validation of measurements of water vapor from the Halogen Occultation Experiment (HALOE), *J. Geophys. Res.*, *101*, 10,205–10,216, 1996.

Holton, J.R., P.H. Haynes, M.E. McIntyre, A.R. Douglass, R.B. Rood, and L. Pfister, Stratosphere- troposphere exchange, *Rev. Geophys.*, *33*, 403–439, 1995.

Jones, R.L., and J.F.B. Mitchell, Is water vapour understood?, *Nature*, *353*, 210, 1991.

Kelly, K.K., A.F. Tuck, and T. Davies, Wintertime asymmetry of upper tropospheric water between the Northern and Southern Hemispheres, *Nature*, *353*, 244–247, 1991.

Larsen, J.C., E.W. Chiou, W.P. Chu, M.P. McCormick, L.R. McMaster, S. Oltmans, and D. Rind, A comparison of the Stratospheric Aerosol and Gas Experiment II tropospheric water vapor to radiosonde measurements, *J. Geophys. Res.*, *98*, 4897–4917, 1993.

Lindzen, R.S., Some coolness regarding global warming, *Bull. Am. Meteorol. Soc.*, *71*, 288–299, 1990.

Manabe, S., and R.T. Wetherald, Thermal equilibrium of the atmosphere with a given distribution of relative humidity, *J. Atmos. Sci.*, *24*, 241–259, 1967.

Mote, P.W., K.H. Rosenlof, M.E. McIntyre, E.S. Carr, J.C. Gille, J.R. Holton, J.S. Kinnersley, H.C. Pumphrey, J.M. Russell III, and J.W. Waters, An atmospheric tape recorder: The imprint of tropical tropopause temperatures on stratospheric water vapor, *J. Geophys. Res.*, *101*, 3989–4006, 1996.

Newell, R.E., Y. Zhu, E.V. Browell, S. Ismail, W.G. Read, J.W. Waters, K.K. Kelly, and S.C. Liu, Upper tropospheric water vapor and cirrus: Comparison of DC-8 observations, preliminary UARS microwave limb sounder measurements and meteorological analyses, *J. Geophys. Res.*, *101*, 1931–1941, 1996.

Newell, R.E., Y. Zhu, W.G. Read, and J.W. Waters., Relationship between tropical upper tropospheric moisture and eastern tropical Pacific sea surface temperature at seasonal and interannual time scales, *Geophys. Res. Lett.*, *24*, 25–28, 1997.

Peixoto, J.P., and A.H. Oort, The climatology of relative humidity in the atmosphere, *J. Clim.*, *9*, 3443–3463, 1996.

Pierrehumbert, R.T., Thermostats, radiator fins, and the local runaway greenhouse, *J. Atmos. Sci.*, *52*, 1784–1806, 1995.

Rasmusson, E.M., Seasonal variation of tropical humidity parameters, in *General Circulation of the Tropical Atmosphere*, vol. 1, edited by R.E. Newell, J.W. Kidson, D.G. Vincent, and G.J. Boer, pp. 193–237, MIT Press, Cambridge, Mass., 1972.

Read, W.G., J.W. Waters, D.A. Flower, L. Froidevaux, R.F. Jarnot, D.L. Hartmann, R.S. Harwood, and R.B. Rood, Upper tropospheric water vapor from UARS MLS, *Bull. Am. Meteorol. Soc.*, *76*, 2381–2389, 1995.

Rind, D., E.-W. Chiou, W. Chu, J. Larsen, S. Oltmans, J.Lerner, M.P. McCormick, and L. McMaster, Positive water vapor feedback in climate models confirmed by satellite data, *Nature*, *349*, 500–503, 1991.

Rind, D., E.-W. Chiou, S. Oltmans, J. Lerner, J. Larsen, M.P. McCormick, and L. McMaster, Overview of the Stratospheric Aerosol and Gas Experiment II water vapor observations: Method, validation, and data characteristics, *J. Geophys. Res.*, *98*, 4835–4856, 1993.

Rosenlof, K.H., A.F. Tuck, K.K. Kelly, J.M. Russell III, and M.P. McCormick, Hemispheric asymmetries in water vapor and inferences about transport in the lower stratosphere, *J. Geophys. Res.*, *102*, 13,213–13,234, 1997.

Russell, J.M. III, L.L. Gordley, J.H. Park, S.R. Drayson, W.D. Hesketh, R.J. Cicerone, A.F. Tuck, J.E. Frederick, J.E. Harries, and P.J. Crutzen, The Halogen Occultation Experiment, *J. Geophys. Res.*, *98*, 10,777–10,798, 1993.

Soden, B.J., and F.P. Bretherton, Interpretation of TOVS water vapor radiances in terms of layer-average relative humidities: Method and climatology for the upper, middle, and lower troposphere, *J. Geophys. Res.*, *101*, 9333–9343, 1996.

Spencer, R.W., and W.D. Braswell, How dry is the tropical free troposphere? Implications for global warming theory, *Bull. Am. Meteorol. Soc.*, *78*, 1097–1106, 1997.

Stone, E.M., W.J. Randel, J.L. Stanford, W.G. Read, and J.W. Waters, Baroclinic wave variations observed in MLS upper tropospheric water vapor, *Geophys. Res. Lett.*, *23*, 2967–2970, 1996.

Udelhofen, P.M., and D.L. Hartmann, Influence of tropical cloud systems on the relative humidity in the upper troposphere, *J. Geophys. Res.*, *100*, 7423–7440, 1995.

Waters, J.W., Microwave Limb Sounding, in *Atmospheric Remote Sensing by Microwave Radiometry*, edited by M. A. Janssen, pp. 383–496, John Wiley, New York, 1993.

W.G. Read and J.W. Waters Jet Propulsion Laboratory, Mail Stop 183–701, 4800 Oak Grove Drive, Pasadena, CA 91109.

K.H. Rosenlof, Cooperative Institute for Research in Environmental Sciences NOAA Aeronomy Laboratory, 325 Broadway, Boulder, CO 80303.

B.J. Sandor (corresponding author), National Center for Atmospheric Research, Atmospheric Chemistry Division, P.O. Box 3000, Boulder, CO 80307-3000. (email: sandor@acd.ucar.edu)